Electronic structure of atomic chains on vicinal Si(111)-Au

K. N. Altmann, J. N. Crain, A. Kirakosian, J.-L. Lin, D. Y. Petrovykh, and F. J. Himpsel
Department of Physics, University of Wisconsin–Madison, 1150 University Avenue, Madison, Wisconsin 53706

R. Losio
Department of Physics, University of Durham, Durham DH1 3LE, United Kingdom
(Received 10 January 2001; published 19 June 2001)

Unusual electronic states are found for gold-induced chain and ladder structures on vicinal Si(111) surfaces, such as Si(111)5×2-Au and Si(557)-Au. As two-dimensional reference the Si(111)$\sqrt{3}\times\sqrt{3}$-Au surface is investigated. The highly stepped Si(557)-Au surface is metallic, despite an even electron count. That is explained by two half-filled, nearly degenerate bands. On the Si(111)5×2-Au surface we find a band that changes continuously from one dimensional at its maximum to two dimensional at its minimum. It exhibits a pseudogap within 0.3 eV of the Fermi level E_F, where the spectral weight is strongly reduced. Si(111)$\sqrt{3}\times\sqrt{3}$-Au exhibits an electron pocket at Γ that changes its filling continuously with increasing Au coverage.

DOI: 10.1103/PhysRevB.64.035406 PACS number(s): 73.20.At, 79.60.Jv, 71.10.Pm

I. INTRODUCTION

Metals on semiconductors generate a large variety of low-dimensional surface structures with interesting electronic properties.[1–9] There have been reports of correlation effects destroying the metallicity of surfaces despite an odd electron count per unit cell,[1,2] of anomalous surface corrugation by charge density waves[3] or by large atomic displacements,[4] of metallic nanowires,[5] of a surface state with mixed dimensionality,[6] of spin-charge separation in a Luttinger liquid,[7,8,10] and of a surface with an even electron count becoming metallic.[9] Theory predicts a variety of exotic phases in such low-dimensional systems, which are generated by the increased interactions and subsequent correlations that electrons experience when they are confined.[1,10] This can be rationalized at the classical level for a one-dimensional system: two electrons approaching each other with opposite velocities along a line cannot avoid penetrating each other, whereas they have an increasing number of ways to escape an encounter in higher-dimensional systems.

Gold on Si(111) exhibits a particularly rich phase diagram containing both one- and two-dimensional structures.[11–15] At the lowest coverage a Si(111)5×2-Au phase is observed that consists of stripes with one-dimensional character (Figs. 1 and 2). With higher coverage several two-dimensional phases are formed, such as two related $\sqrt{3}\times\sqrt{3}$ structures (Fig. 2), and eventually a 6×6 structure that consists of an ordered array of $\sqrt{3}\times\sqrt{3}$ domains.[11] Beyond flat Si(111) there are opportunities for using stepped Si(111) surfaces to produce tailored, one-dimensional structures with exotic electronic states, as demonstrated in Refs. 7 and 9. Low step densities with a miscut angle of about 1° stabilize a single domain of the one-dimensional 5×2 structure. High miscut angles, such as 9.5° for Si(557),[7,9,16,17] create a whole new category of one-dimensional structures that incorporate a step into the unit cell (Fig. 1). Several of the structures induced by Au on flat and stepped Si(111) have been reported to be metallic,[7,9,18,19] which is the exception rather than the rule at semiconductor surfaces. That opens the possibility for creating some of the more exotic low-dimensional phases, such as the Luttinger liquid.[7,10]

One-dimensional structures of Au on Si(111) give a nice example of the options for tailoring electronic states. Table I shows how the number of atomic chains can be modified by adding steps and by varying the Au coverage. That affects the electron count in the unit cell and is critical for metallic versus insulating character. The Si(111)5×2-Au surface contains two rows of Au atoms separated by a single Si row spacing, according to transmission electron microscopy and diffraction.[12] The highly stepped Si(557)-Au surface has a comparable unit cell of $5\frac{2}{3}$ rows when projected onto the (111) plane. It contains only one row of Au atoms, plus a step. Furthermore, chains with a doubled spacing of the atoms along the chain are observed by scanning tunneling microscopy (STM). These chains might be formed by Si adatoms. The Si(111)5×2-Au surface contains one such chain per unit cell,[13] and the Si(557)-Au two chains with a spacing of two rows.[9] The electron count differs in these two structures as well, as long as one considers an $(n\times1)$ unit cell without period doubling along the chains.[9] The Si(557)-Au surface with an even count is metallic and seems to defy conventional wisdom that an even electron count produces a semiconductor and an odd count a metal. Si(111)5×2-Au, on the other hand, exhibit a pseudogap where a band abruptly loses spectral weight before reaching the Fermi level.

We focus on these one-dimensional chain structures of gold on flat and stepped Si(111) and compare them with a two-dimensional structure, the Si(111)$\sqrt{3}\times\sqrt{3}$-Au reconstruction. Their topography is characterized by STM as shown in Fig. 2. Indeed, we find one-dimensional chains for Si(111)5×2-Au and Si(557)-Au, and a two-dimensional, triangular array for Si(111)$\sqrt{3}\times\sqrt{3}$-Au. STM is also a critical indicator of the surface quality and facilitates optimizing the growth conditions. Angle-resolved photoemission is used to map out the electronic structure, particularly the low-

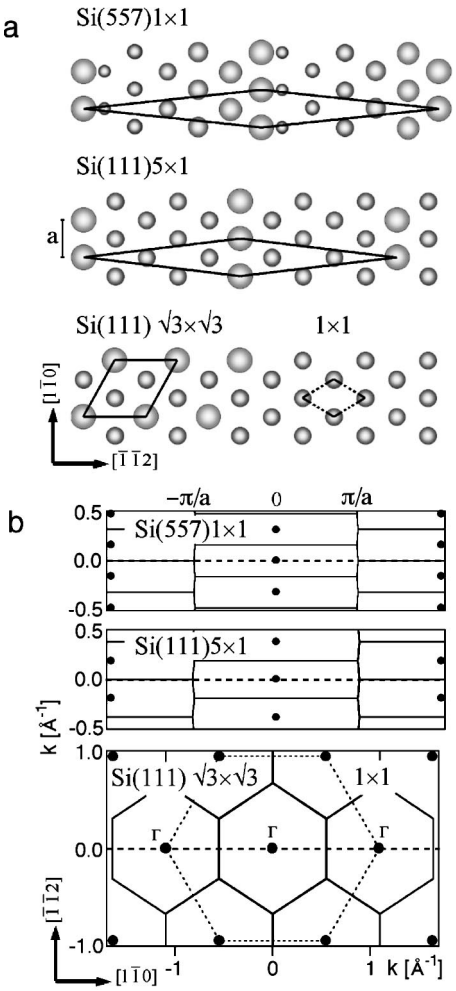

FIG. 1. Overview of the unit cells for the three structures of Au on Si discussed here, both in real space (a) and in reciprocal space (b). The chains and steps are running in the $[1\bar{1}0]$ direction with a period $a = a_{cubic}/\sqrt{2} = 3.84$ Å along the chains.

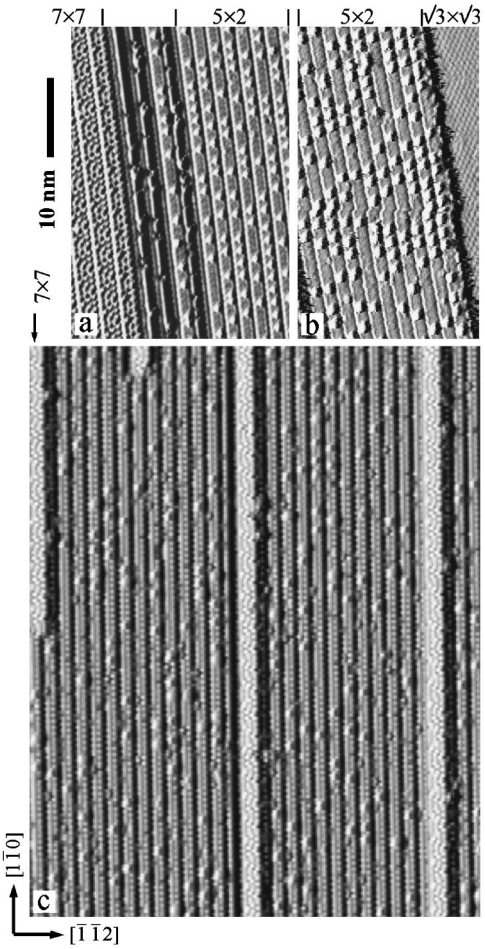

FIG. 2. Optimization of surfaces and coverage calibration using STM. The Au coverage for flat Si(111)5×2-Au is twice as large as for stepped Si(557)-Au (0.4 ML versus 0.2), indicating two Au rows versus one. (a) Si(111)5×2-Au: Insufficient Au coverage leads to patches of clean 7×7. (b) Si(111)5×2-Au: Excess Au coverage leads to patches of $\sqrt{3}\times\sqrt{3}$-Au. (c) Si(557)-Au: Insufficient Au coverage leads to Si(111)7×7 stripes one unit cell wide. The *x* derivative of the STM topography is shown, giving the appearance of illumination from the left with steps casting shadows to the right. The sample bias is −1 V for (a) and (b), and +2 V for (c).

dimensional states in the band gap of the Si substrate. A high-resolution spectrometer with energy and angle multidetection allows us to zoom in on the band dispersion near the Fermi level that determines metallic behavior and the tendency toward electronic phase transitions, such as charge density waves or more exotic phases.

In Sec. II we first explain the preparation of highly ordered surfaces with well-defined structures. The annealing sequence and the correct gold coverage turn out to be critical for obtaining optimum surfaces. The route is determined by STM coupled with low-energy electron diffraction (LEED). These findings are confirmed by coverage-dependent photoemission spectra of the surface states and the Si 2*p* core level. The cross section of the surface states in photoemission is optimized by varying the photon polarization and the photon energy, and by choosing higher Brillouin zones. Section III gives an overview of the photoemission results of the surface states for three well-defined surface structures. Si(557)-Au and Si(111)5×2-Au are chainlike, whereas Si(111)$\sqrt{3}\times\sqrt{3}$-Au provides a two-dimensional reference. Sections IV and V discuss the physics of the one- and two-dimensional surfaces in detail. Rather unusual properties are observed, such as two nearly degenerate surface state bands on Si(557)-Au that give a metallic surface despite an even electron count per unit cell. A continuous transition from two-dimensional to one-dimensional behavior is observed

TABLE I. Properties of one-dimensional Au chain structures on flat Si(111) and stepped Si(557).

	Si(111)-Au	Si(557)-Au
Unit cell in rows	5	$5\frac{2}{3}$
Steps	0	1
Au chains	2	1
Double-spaced chains	1	2
Electron count ($n\times1$)	odd	even

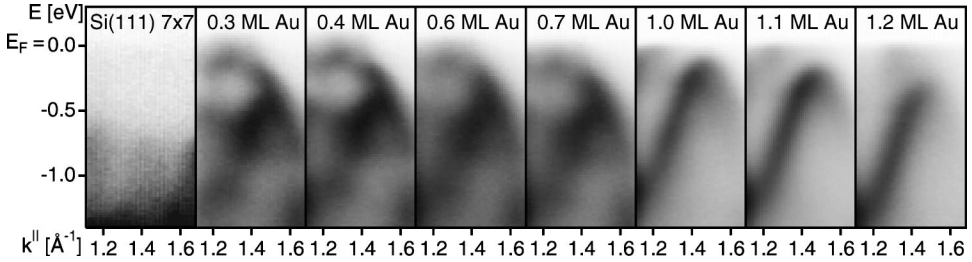

FIG. 3. Coverage dependence of the surface bands for Au on Si(111). Two distinct patterns are observed that correspond to Si(111) 5×2-Au and Si(111) $\sqrt{3}\times\sqrt{3}$-Au with a coverage of 0.3–0.7 and 1.0–1.2 ML, respectively. Dark features in the $E,k^{||}$ distributions represent high photoemission intensity.

for a surface state on Si(111)5×2-Au. This surface also exhibits a pseudogap near the Fermi level at low temperature. The two-dimensional Si(111) $\sqrt{3}\times\sqrt{3}$-Au surface exhibits an interesting interference pattern with the projected bulk bands. Section VI summarizes our findings and points out future directions for designing low-dimensional structures with tailored electronic features on vicinal surfaces.

II. SURFACE CHARACTERIZATION BY STM, LEED, AND PHOTOEMISSION

For preparing surface structures with optimum uniformity and ordering we found the stoichiometry and the annealing sequence to be the most critical parameters. First, we will address the calibration of the optimum Au coverage by LEED, STM, and photoemission, and then describe the optimum annealing sequences and their rationale. The technical details of the photoemission experiment will be described at the end of this section.

As definition for the Au coverage we use units of Si(111) atomic layers [1 ML (monolayer) $=7.8\times10^{14}$ atoms/cm^2]. According to previous work, Si(111)5×2-Au contains 0.44 ML per unit cell,[14] close to two Au rows out of five rows in the unit cell. Likewise, it has been determined that Si(557)-Au contains 0.20 ML of Au per unit cell,[7,16] which corresponds to about a single Au row for the $5\frac{2}{3}$ rows of the (557) unit cell. The number of Au rows is rounded to the next integer in view of our uncertainty of ±0.05 ML in the absolute calibration. The Si(111) $\sqrt{3}\times\sqrt{3}$ structure exists near 1 ML Au coverage and comes in two varieties (α at low coverage, β at high coverage), as indicated by the fine structure of the diffraction spots[11,12] and by Si $2p$ core levels at the surface.[15]

The most accurate determination of the optimum coverage for each phase is achieved by STM, as shown in Figs. 2(a) and 2(b) for flat Si(111) and Fig. 2(c) for highly stepped Si(557). For example, the coverage in Fig. 2(c) is only 0.02 ML below the optimum. On Si(111)5×2-Au we observe 7×7 patches at suboptimal coverage [Fig. 2(a)], and $\sqrt{3}\times\sqrt{3}$-Au patches beyond the optimum [Fig. 2(b)]. On Si(557) we observe 7×7 patches as well at suboptimal coverage, but they are only a single 7×7 unit cell wide [Fig. 2(c)]. In addition, we find that the clean Si(557) surface is composed of triple steps and triple terraces,[17] which have to be converted to single steps and terraces by the Au. Beyond the optimum coverage we observe terraces combined with bunched steps on Si(557). Our findings confirm the ratio of 2:1 of the Au coverage between Si(111)5×2-Au and Si(557)-Au reported in the literature.[7,9,11,12,16]

LEED observations are in line with the STM results. Less than 0.4 ML of Au produces an admixture of 7×7 spots to the 5×2 spots on flat Si(111), and excess of Au gives rise to an admixture of $\sqrt{3}\times\sqrt{3}$ to 5×2. For practical purposes, LEED of the Si(111)5×2-Au structure is the preferred technique for calibrating the Au evaporator.

In photoemission we observe distinct signatures of the various phases as well, which are shown in Fig. 3 for flat Si(111). These are photoemission intensity distributions in E and $k^{||}$ which reflect the $E(k^{||})$ band dispersions. The surface bands go through two characteristic patterns when the coverage is increased. These are assigned to the 5×2 and $\sqrt{3}\times\sqrt{3}$ phases. As representative for the two phases we have chosen the data at 0.4 ML and at 1.1 ML in subsequent figures. The actual coverage could be less than the nominal values because excess gold agglomerates into three-dimensional islands during multiple 850 °C postanneals. The Si $2p$ core level spectra exhibit two distinct phases as well (not shown), which are consistent with previously reported Si $2p$ data.[15]

The preparation of clean Si substrates with well-defined step structure follows specific heating sequences that we established previously by STM.[17,20] A clean Si surface is obtained by flashing to 1260 °C for 10 s where the native oxide evaporates and residual surface carbon diffuses into the bulk. A quench to a temperature below the 1×1 to 7×7 phase transition at 870 °C avoids step bunching, and a long post-anneal at 850 °C develops long-range 7×7 domains. Gold was deposited at 650 °C substrate temperature with a subsequent anneal at 950 °C. Most of the data were taken at a temperature of 100 K with frequent recleaning at 850 °C, but we also report data taken at 16 K and at 300 K.

The samples were n-doped Si strips, 0.02 Ω m for Si(111) and 1 Ω cm for Si(557). The (111) substrates had an intentional miscut of 1° toward $[\overline{112}]$ in order to obtain single-domain Si(111)5×2-Au surfaces. The Si(557) surface corresponds to a much larger miscut of 9.5° toward $[\overline{112}]$. Narrow Si strips were clamped at their ends to a closed-cycle He refrigerator between sapphire plates and Ta contact sheets for resistive heating. The heating current (dc)

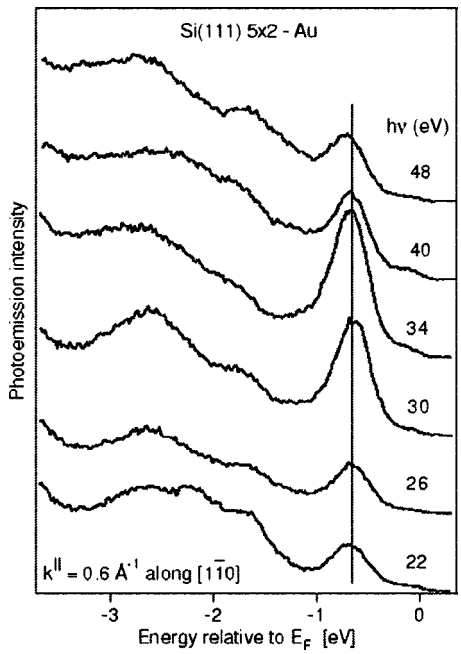

FIG. 4. Surface state photoemission spectra section versus photon energy $h\nu$ for Si(111)5×2-Au at constant $k^{||}$. The lack of dispersion with changing $h\nu$ shows that there is no admixture of bulk states. A maximum in the surface/bulk emission ratio is observed near $h\nu=34$ eV, which is used in the subsequent figures.

was passed parallel to the steps in order to avoid electromigration effects.

Photoemission data were acquired with a hemispherical Scienta SES200 spectrometer equipped with angle and energy multidetection and coupled to an undulator beamline at the Synchrotron Radiation Center (SRC) of UW-Madison. The emission angle θ of the photoelectrons from the surface normal was measured along the $[1\bar{1}0]$ azimuth, which is parallel to the steps. The energy resolution was 20 +7 meV (photons+electrons); the angular interval was 1/4° with multidetection over 12° along the step direction. A larger angular range was covered by rotating the sample in increments of 6°. The angle between the incoming photons and the axis of the electron spectrometer was kept fixed at 50°. All measurements were performed with *p*-polarized light in the emission plane, which contained the chains.

Photon energies in the range 22 eV$\leqslant h\nu \leqslant$48 eV were used in order to demonstrate that there is no coupling to bulk states, which would manifest itself by a change of band energies with changing $h\nu$ at fixed parallel momentum $k^{||}$. Figure 4 shows such a set of photoelectron spectra versus photon energy. Although the peak energy does not change significantly with $h\nu$, the intensity of the surface states varies and exhibits a maximum around $h\nu=34$ eV. A similar behavior was found for clean Si(111)7×7.[21] Our band structure measurements take advantage of this enhancement by using a photon energy $h\nu=34$ eV.

The matrix element for photoemission causes large-scale intensity variations for these surfaces.[21] In particular, there is a dramatic intensity difference between positive and negative $k^{||}$, despite the fact that the $E(k^{||})$ band dispersions should be identical (Fig. 5). The variations are caused by the polarization vector **A** in the dipole matrix element $\langle\psi_f|\mathbf{A}\cdot\mathbf{p}|\psi_i\rangle$. Opposite directions of $k^{||}$ correspond to different directions of **A** relative to the surface normal. The perpendicular component dominates at large positive $k^{||}$ and the parallel component at large negative $k^{||}$. This variability allows us to selectively enhance bands with different wave functions. By the same token, the measurement geometry needs to be taken into account when comparing our data with previous spectra, such as those in Refs. 7 and 9 for Si(557)-Au, in Ref. 18 for Si(111)5×2-Au, and in Ref. 19 for Si(111)$\sqrt{3}\times\sqrt{3}$-Au. In order to reduce variations of the matrix element over large distances in $k^{||}$ we have applied a weak high-pass filter to the data in Fig. 5. For a comparison with the raw data see Figs. 3 and 7, 8, and 9 below.

III. OVERVIEW OF THE SURFACE STATE BANDS

A summary of the surface states observed for the three Si-Au surfaces is given in Figs. 5 and 6. Figure 5 shows the experimental $E(k^{||})$ distributions, and Fig. 6 distills the $E(k^{||})$ dispersions of the most prominent features. These band dispersions are taken along the $[1\bar{1}0]$ azimuth which corresponds to the horizontal dashed lines in Fig. 1(b). The data cover the first and second Brillouin zones in $k^{||}$. For the two chain structures the cuts through the first and second Brillouin zones are not equivalent to each other, with the former passing through the center and the latter along the boundary. They become equivalent in the truly one-dimensional limit where the dispersion perpendicular to the chains vanishes.

Among the three band structures in Fig. 5 the Si(557)-Au bands clearly distinguish themselves by simplicity. At first glance, one sees a half-filled band with its bottom near $\pm\pi/a$, which corresponds to the zone boundary in the one-dimensional limit. Closer inspection reveals two nearly degenerate bands,[22] one slightly more than half filled, the other slightly less (Figs. 7 and 8 and Table II. That explains why a surface with an even electron count has become metallic (see Table I and Ref. 9). The two bands can be accounted for naturally[9] by having two identical orbitals within the unit cell that form bonding (symmetric) and antibonding (antisymmetric) wave functions.

The surface bands of Si(111)5×2-Au are a lot more complex than for Si(557)-Au. Nevertheless, restricting ourselves to the first Brillouin zone between $\pm\pi/a$ we find a single, strong band S_1 that resembles the pair of half-filled bands S_{1A}, S_{1B} on Si(557)-Au. The main difference is a rigid, downward shift by 0.3 eV. The band appears to terminate abruptly at the point of half filling ($ZB^{n\times2}$), leaving a 0.3 eV pseudogap below the Fermi level (Figs. 7 and 9). Of course, a band cannot simply vanish in the middle of the Brillouin zone. It may fold back at the new zone boundary $ZB^{n\times2}$ that is created by period doubling from 5×1 to 5×2. For example, a Peierls transition would create such an effect. Surprisingly, neither the direct continuation of the band toward E_F nor a back-folded branch with significant intensity in the first Brillouin zone is seen. The puzzle becomes more com-

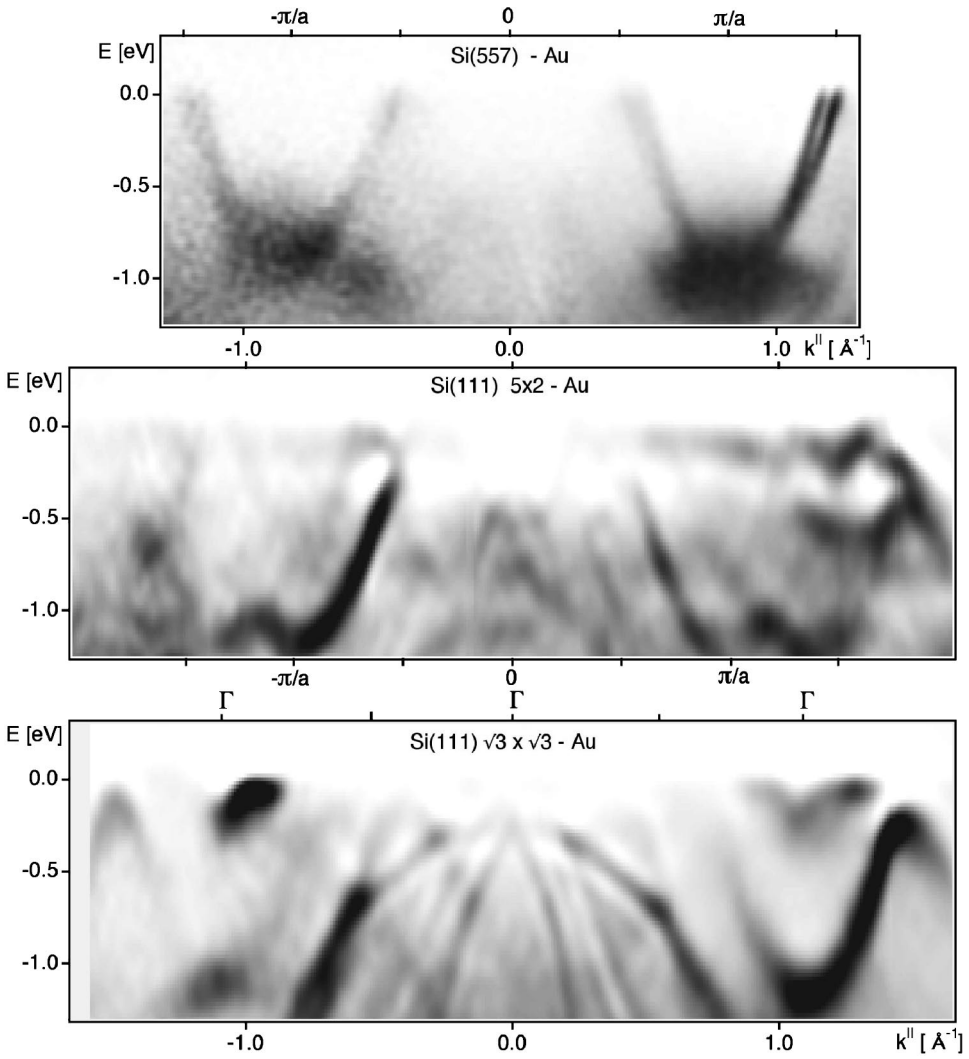

FIG. 5. $E(k^{\|})$ band dispersions of surface states along the $[1\bar{1}0]$ direction, which is parallel to the chains. The Brillouin zones are given in Fig. 1(b). High photoemission intensity is shown dark. The right/left asymmetry is due to different polarization of the photons, with the perpendicular component of **A** large at positive $k^{\|}$.

plex when we look in the second Brillouin zone, where a complicated maze of bands appears, some of them reaching all the way to the Fermi level.

The strongest surface state band of the Si(111) $\sqrt{3}\times\sqrt{3}$-Au surface (S_2 in Fig. 6) resembles the main band on the Si(111)5×2 surface (S_1), but it is shifted in k to accommodate the different Brillouin zone of this two-dimensional structure. Instead of being centered at the zone boundary, the band is now symmetric about the center Γ of the second zone of the $\sqrt{3}\times\sqrt{3}$ structure. The gap below E_F remains similar to that for Si(111)5×2 (about 0.3 eV). It is filled in by a second band (S_1) that renders the $\sqrt{3}\times\sqrt{3}$ surface metallic. It creates a small electron pocket at Γ that resembles a state found on Si(111) $\sqrt{3}\times\sqrt{3}$-Ag,[23,24] including the peculiarity that it is not visible at the Γ point of the first Brillouin zone ($k^{\|}=0$).

In addition to the surface bands we find two bands near $k^{\|}=0$ on Si(111) $\sqrt{3}\times\sqrt{3}$-Au that track the edges of the heavy and light hole bands of bulk Si (see B_1, B_2 in Fig. 6). Their band dispersion is two dimensional, however, since it does not change when varying the photon energy. Furthermore, they split into several subbands (Fig. 5). Although these bands become more pronounced at higher Au coverage they cannot be due to Au states. The Au(111) islands that are expected to form on top of Si(111) $\sqrt{3}\times\sqrt{3}$-Au have a band gap at $k^{\|}=0$ that extends from E_F down to $E_F-1.1$ eV.[25] Possible explanations of this phenomenon and the relation to quantum well states will be explored in Ref. 26.

The dominant surface and bulk features are fitted by parabolic bands, and by higher-order polynomials for S_2, S_3 on Si(111) $\sqrt{3}\times\sqrt{3}$-Au. These are determined by fitting peaks in the momentum distribution of the photoemission intensity $I(k^{\|})$ at fixed energy E. Band maxima and minima are obtained from energy distributions $I(E)$ at fixed $k^{\|}$. The result is displayed in Fig. 6 in order to give a concise presentation of the dominant surface bands. Critical points, effective masses, and Fermi velocities are extracted from these fits and compiled in Table II. In the following sections we discuss possible models of the band topology for each surface separately and address the question of the orbital character of the surface states. Despite a substantial body of structural work there is no agreement on the atomic arrangement of the one-dimensional chain structures yet. That has hampered theoretical efforts to explain the surface electronic structure. Our findings narrow down the choices significantly and make a first step toward understanding the origin of these exotic, low-dimensional bands.

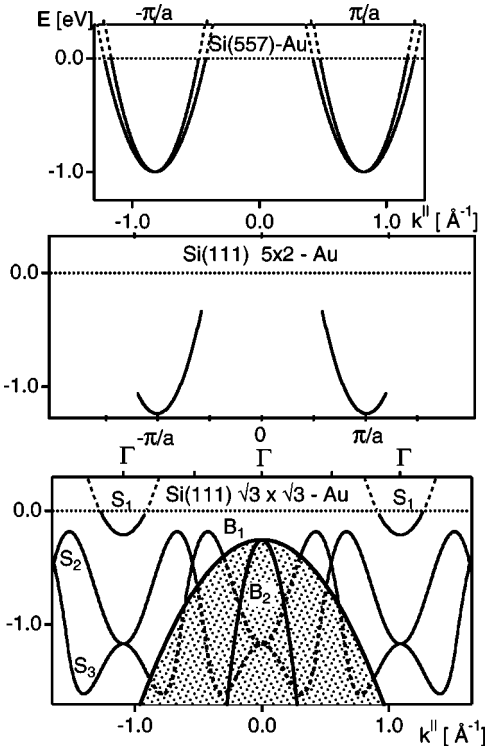

FIG. 6. Fit curves to the dominant surface state bands observed in Fig. 5, including the projected bulk bands observed on Si(111)$\sqrt{3}\times\sqrt{3}$-Au (hatched). Note that the panel for Si(111) $\sqrt{3}\times\sqrt{3}$-Au extends to lower energy than the data in Fig. 5.

IV. CHAIN STRUCTURES: SI(557)-AU AND Si(111)5×2-Au

A. Common features

The Si(557)-Au and Si(111)5×2-Au structures have common features, such as one-dimensional chains. Their basic electronic characteristics are quite different, however. As shown in Table I, they differ in the Au coverage, the number of chains, and the electron count.

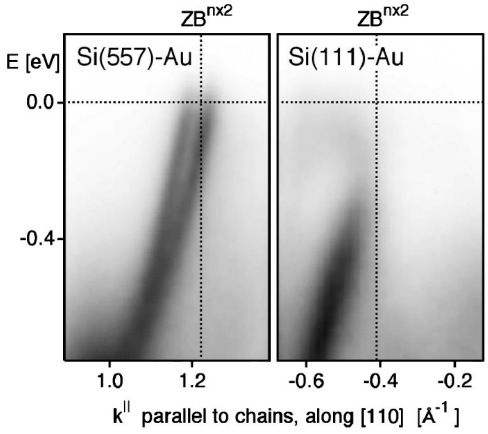

FIG. 7. Band dispersion $E(k^{\|})$ near the Fermi level for the two chain structures. Si(557)-Au is truly metallic with a pair of half-filled bands, whereas Si(111)5×2-Au exhibits a pseudogap below E_F. $ZB^{n\times 2}$ is the point of half filling, which becomes the zone boundary after doubling the period along the chains.

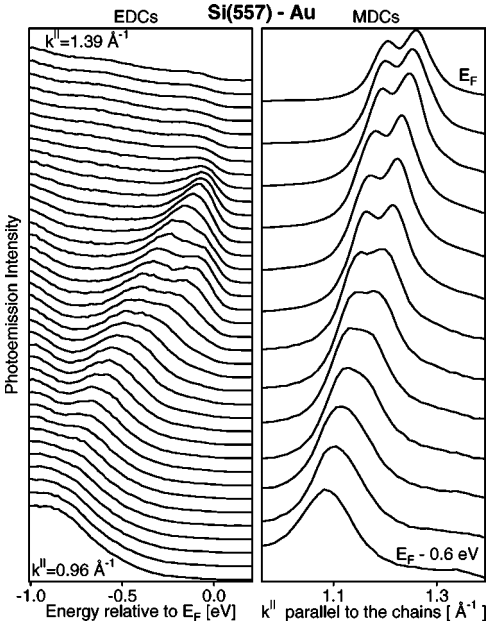

FIG. 8. Decomposition of the Si(557)-Au band dispersion into energy distribution curves (EDC's) and momentum distribution curves (MDC's), which correspond to vertical and horizontal cuts in Fig. 7 (left). The finite splitting at E_F is clearly visible in the MDC's, but somewhat obscured by the Fermi cutoff in the EDC's.

TABLE II. Critical points of surface states (S) and bulk bands (B) along the $[1\bar{1}0]$ azimuth (see Fig. 6). Minima (min), maxima (max), and Fermi level crossings (F) of the bands are given. Energies E are in eV relative to the Fermi level E_F, wave vectors k in Å^{-1} (reduced to the first Brillouin zone), effective masses m_{eff} in units of the free electron mass, and Fermi velocities v_F in 10^6 m/s.

State	E	k	m_{eff}	v_F
		Si(557)-Au		
$S_{1A}^{\min}=S_{1B}^{\min}$	−1.0	0.82	0.45	
S_{1A}^{F}	0	0.38		1.0
S_{1B}^{F}	0	0.44		1.0
		Si(111)5×2-Au		
$S_1^{\min}$	−1.25	0	0.51	
$S_1^{\max}$	−0.3	0.41		
		Si(111)$\sqrt{3}\times\sqrt{3}$-Au [a]		
$S_1^{\min}$	−0.21	0	0.59	
S_1^{F}	0	0.18		−0.35
$S_2^{\max}$	−0.20	0.42		
$S_2^{\min}$	−1.2	0	0.32	
$S_3^{\max}$	−1.2	0	−0.42	
$S_3^{\min}$	−1.6	0.32		
$B_1^{\max}$	−0.25	0	−2.4	
$B_2^{\max}$	−0.25	0	−0.2	

[a]The energies are for a Au coverage of 1.1 ML, as shown in Figs. 5 and 6. For 1.0 ML coverage, all energies are 0.04 eV higher, and for 1.2 ML 0.13 eV lower, due to different filling of the S_1 electron pocket.

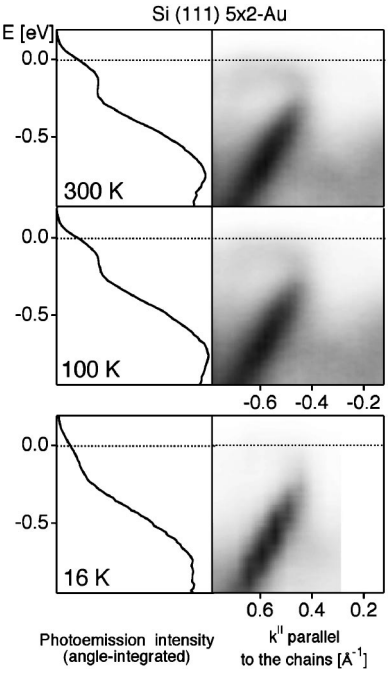

FIG. 9. Temperature dependence of the pseudogap of the S_1 band for Si(111)5×2-Au. The band dispersion $E(k^{||})$ and the angle-integrated spectrum both exhibit a drop of the spectral weight at 0.3 eV below E_F.

To obtain the electron count we begin with an unreconstructed Si(557)1×1 and Si(111)5×1 surface in Fig. 1(a) and then consider the effect of reconstruction, such as addition or removal of Si atoms and doubling of the period along the chains. Si(111)5×1 has five surface atoms in the unit cell, each with a single unpaired electron in a broken bond. Si(557)1×1 contains a total of seven unpaired electrons, five terrace atoms with a single broken bond plus a step atom with two broken bonds (see Ref. 16 for a side view of the structure and Ref. 9 for a more realistic step edge containing an extra row of second layer atoms). Next, we include Au atoms with an unpaired *s* electron, one Au for Si(557)1×1 and two for Si(111)5×1 according to the coverage of one and two Au rows. That adds up to eight electrons for Si(557)-Au and seven for Si(111)5×1-Au. Finally, silicon atoms may be incorporated or removed during reconstruction, e.g., by introducing Si adatoms or making room for Au atoms. Since a Si atom contains four electrons it does not affect the parity of the electron count. After doubling the unit cell along the chain direction both surfaces exhibit an even electron count. Extra atoms observed on top of the chains might contribute a small, fractional electron count to these integers.[28]

A doubling of the period along the chain is observed by STM for both Si(557)-Au and Si(111)5×2-Au. Two double-spaced chains are found on Si(557)-Au [see Fig. 3 in Ref. 9 and Fig. 2(c) here], and one such chain is observed on Si(111)5×2-Au (see Figs. 4 and 9 in Ref. 13). Adjacent chains lack phase correlation, an effect similar to that observed for the Si(111)4×2-In chain structure.[5] Such disorder leads to faint streaks at the half-order positions in diffraction experiments.[11,12,27] We find that a Fourier transform of our STM images gives the same half-order streaks. These extend almost throughout the Brillouin zone in the direction perpendicular to the chains. The effect on the photoemission spectra would be a small probability of transferring half-order $k^{||}$ vectors to the final state wave function, which is a time-reversed LEED state. A well-defined $\delta k^{||}=\pm\pi/a$ would be transferred along the $[1\bar{1}0]$ direction, combined with nearly arbitrary δk perpendicular to the chains. We see no evidence of such a $k^{||}$ transfer, which would give rise to a back-folding of the bands about the new $(n\times2)$ zone boundaries at $k^{||}=\pi/2a$. Therefore, we have omitted half-order reciprocal lattice vectors in the Brillouin zones in Fig. 1(b).

The Brillouin zones of the Si(557)-Au and Si(111) 5×2-Au chain structures are quite similar [Fig. 1(b)]. The average zone boundary in the $[1\bar{1}0]$ direction is at $\pi/a=0.82$ Å^{-1} for both, where $a=3.84$ Å is the atomic spacing along the chains [Fig. 1(a); $a=a_{cubic}/\sqrt{2}$]. Perpendicular to the chains we have a period $2\pi/d$ which corresponds to a chain spacing $d=19.1$ Å for Si(557) and $d=16.6$ Å for Si(111)5×2.

The bands of the two chain structures appear to be related, as long as we restrict ourselves to the first Brillouin zone. In both cases we observe a dominant band that is about 1.0 eV wide and extends from a minimum at the zone boundary $\pm\pi/a$ to the point of half filling at $\pm\pi/2a$. There are two differences: The Si(557)-Au band splits into a pair (S_{1A} and S_{1B}), and the Si(111)5×2-Au band is shifted down by 0.3 eV, leaving a pseudogap with reduced spectral weight at the Fermi level (Figs. 7 and 9). In the second Brillouin zone beyond $\pm\pi/a$ the two surfaces behave very differently. For Si(557)-Au the bands continue as mirror images about the zone boundary $\pm\pi/a$, whereas a complicated set of new bands appears for Si(111)5×2-Au. Some of these come very close to the Fermi level near $+1.3$ Å^{-1}. A similar region of intense emission near E_F was reported in Ref. 18 and used as evidence for metallic character. Even though these extra bands lie suspiciously close to the S_1,S_2 bands of Si(111)$\sqrt{3}\times\sqrt{3}$-Au, it is unlikely that they are caused by $\sqrt{3}\times\sqrt{3}$ patches on the 5×2 surface, such as those shown in Fig. 2(b). The stability of these bands down to lower Au coverage in Fig. 3 suggests otherwise. A set of common bands between the 5×2 and $\sqrt{3}\times\sqrt{3}$ structures could simply be an indication that they have common arrangements of local orbitals. These bands are centered about the Γ point in the second $\sqrt{3}\times\sqrt{3}$ Brillouin zone, which coincides with the corner of the 1×1 Brillouin zone [see Fig. 1(b)]. That point is relevant to both structures because it is a special point for the projected bulk bands that delineate the E,k regions available for surface states.

Going deeper into the orbital character of the bands is not easy in view of the scarce information about the atomic structure and the absence of band calculations. There is no structure analysis of Si(557)-Au, such that we have to rely on our STM images as the main source of structural information [Fig. 2(c) here and Fig. 3 in Ref. 9]. Several structural models have been proposed for Si(111)5×2-Au, with recent transmission electron microscopy and diffraction data[12] supporting two single-spaced Au rows with slight atomic dis-

placements, plus a double-spaced row of Si adatoms. Despite these uncertainties, we make our best effort to expose the intriguing questions that arise if one tries to construct a picture that is consistent with the electron count and the chain structure.

B. Si(557)-Au bands

As our best interpretation of the Si(557)-Au data we propose a closely spaced doublet of metallic, half-filled bands (S_{1A},S_{1B}). These bands lie very close to the two bands reported in Ref. 7, particularly when viewed in a similar way as EDC's (Fig. 8, left panel). The MDC's in Fig. 8 clearly reveal that the band splitting does not vanish at E_F (Fig. 8, top curve of the right panel). In fact, the splitting increases when approaching E_F. That immediately rules out the previous interpretation as the spinon-holon splitting of a Luttinger liquid.[7] Spinon and holon bands have to converge at E_F.[10] Furthermore, having just a single band cross the Fermi level would not be compatible with the even electron count. The same argument rules out other splitting mechanisms for a single band, such as a spin splitting.[29] The observed metallicity is quite unusual in view of the even electron count. In fact we are not aware of any other semiconductor surface with such a doublet of half-filled bands.

Two nearly degenerate energy bands suggest two nearly identical orbitals within the unit cell. When these interact they generate even/odd combinations of the individual wave functions with bonding/antibonding character. The two orbitals may originate from a single chain with two orbitals per atom or from two chains. In the first case one could have a set of in-plane, $p_{x,y}$-derived orbitals, such as the two broken bonds of the step edge atoms or the orbitals connecting a zig-zag chain. The second case would match our observation of two chains per unit cell in the STM images [Fig. 2(c) here and Fig. 3 in Ref. 9]. If we considered these chains as consisting of Au atoms we would obtain the correct Au coverage (two double-spaced chains give one Au row), but would have a difficult time explaining why the bands are not backfolded at $\pm\pi/2a$ with a resulting gap at E_F.

Alternatively, one could assign Si atoms instead of Au to the observed double-spaced chains and argue that there are two additional, single-spaced chains that produce the two bands seen in photoemission. An assignment of the observed double-spaced chains to Si adatoms looks attractive since the observed 2×2 and $c(4\times2)$ patterns of adjacent chains[9] match the 2×2 and $c(4\times2)$ adatom structures on Si(111). In this case one would expect two sets of bands, an empty band at about $+0.6$ eV for the adatoms and a full band at about 0.9 eV for the rest atoms.[21,30] Adatoms transfer their unpaired electrons to the rest atoms and allow them to form a stable lone pair.

An interesting combination of chains has come up in first-principles calculations[31] of model chain structures for Si(557)-Au. Having a single Au chain between two chains of Si atoms produces a pair of energy bands similar to those observed in photoemission. These bands are associated with Si atoms. Si transfers an electron to the Au, where it pairs up with the single Au $6s$ electron to form a stable state well below E_F. A variety of chain structures is currently under consideration by first-principles calculations of the total energy and the band structure.[31,32]

The concept of double-spaced Si chains combined with single-spaced metallic chains is consistent with spectroscopic STM observations. The empty adatom band explains the double periodicity observed at positive sample bias [$+2$ V in Fig. 2(c)]. STM from filled states produces continuous lines along the chains, which is consistent with an assignment of the pair of half-filled bands to unresolved single-period chains. For example, Fig. 2(a) with a sample bias of -1 V contains a few unit cells of Si(557)-Au in the transition region between 7×7 and 5×2-Au. They consist of structureless chains, while the 2×2 subunits of the 7×7 patch are well resolved. The situation is similar for Si(111)5×2-Au, where STM shows a doubled period for empty states but a continuous line for filled states (see Fig. 8 in Ref. 13).

C. Si(111)5×2-Au bands

The Si(111)5×2-Au bands generate at least three puzzles. First, there is the question of the origin of the metallic bands in the second Brillouin zone. Second, the dispersion of the dominant band S_1 ends abruptly at 0.3 eV below E_F without a clear continuation (see Figs. 7 and 9). Third, the S_1 band changes continuously from one dimensional at its maximum to two dimensional at its minimum, as reported in detail previously.[6] Question 1 was described already in Sec. III. In the following we comment on questions 2 and 3.

In Figs. 7 and 9, the dominant band S_1 of Si(111) 5×2-Au suddenly loses spectral weight at $\pm\pi/2a$, the $k^{||}$ point where a half-filled band is expected to cross the Fermi level. However, the band has not reached E_F yet and appears to leave a gap of 0.3 eV below E_F. We refer to this gap as a pseudogap because the spectral weight does not vanish completely. Possible sources of the residual spectral weight are the metallic bands in the second Brillouin zone and a lattice gas of extra atoms on top of the chains.[28] A gap at $\pm\pi/2a$ is not surprising by itself since the observed period doubling along the chains creates an extra zone boundary at $k^{||}=\pm\pi/2a$ (labeled $\mathrm{ZB}^{n\times2}$ in Fig. 7). In fact, the canonical prediction for a one-dimensional metal is a Peierls transition toward an insulator with a gap forming exactly at that point. However, the observed pseudogap of 0.3 eV is much larger than expected from a Peierls transition. The temperature dependence in Fig. 9 shows a reduction of the spectral weight inside the pseudogap at low temperatures, not a change of the gap, as one might expect at a phase transition. That is consistent with the size of the gap, which is far greater than kT for our temperature range. Such a large gap can be rationalized by the natural tendency of the Si(111) surface to create adatom structures with a doubled unit cell. The lattice distortion is much larger than for a Peierls distortion in this case. Nevertheless, the suppression of back folding for the S_1 band (see Fig. 5 inside $\pm\pi/2a$) is surprising for such a strong distortion. Electron correlations might provide an alternative explanation for a large gap. Such a mechanism has

been invoked for explaining the insulating behavior of other Si(111) surfaces with an odd electron count.[1,2,8]

Measurements of the band dispersion of S_1 perpendicular to the chains[6] show that it is one dimensional at the top and becomes gradually two dimensional further down in energy. Such unusual behavior can be explained intuitively by a mechanism that decouples the chains at a particular $k^{||}$ point by placing a node of the wave function on the atoms that couple the chains.[6] This can be cast into quantitative form by a tight binding Hamiltonian that contains not only a coupling t_1 along the chains and a perpendicular coupling t_2, but also a diagonal coupling t_3 (for details see Ref. 33). Essentially, t_2 and t_3 are able to compensate each other at a particular $k^{||}$ point and eliminate the dispersion perpendicular to the chains at that point.

V. TWO-DIMENSIONAL Si(111) $\sqrt{3}\times\sqrt{3}$-Au

The Si(111) $\sqrt{3}\times\sqrt{3}$-Au surface not only serves as a two-dimensional reference, but also has an interesting band structure in its own right. Well-defined electron pockets make it metallic, and a pair of equivalent bands produces a special band topology. Beyond that we find an intricate interference pattern that replicates the bulk bands (for details see Ref. 26).

Si(111) $\sqrt{3}\times\sqrt{3}$-Au shows three surface bands in the energy range considered here, two of them equivalent. For all three we observe minima at the Γ points in the second Brillouin zone. These are located at $k^{||}=1.09$ Å^{-1}, which is 4/3 times the Brillouin zone boundary π/a of the chain structures. The equivalent Γ point in the first zone is obscured by the projected bulk bands. Those can be directly observed on this surface (Fig. 5 and Fig. 6, hatched area).

The uppermost surface state S_1 forms an electron pocket centered at Γ that makes the Si(111) $\sqrt{3}\times\sqrt{3}$-Au structure metallic. A similar pocket has been observed for Si(111) $\sqrt{3}\times\sqrt{3}$-Ag and related structures where extra Ag and Au atoms donate electrons to the surface state band and move the Fermi level up in the band.[23] These states have also been used to explain an increase in the surface conductance versus coverage.[24] We find a similar change in the occupancy of the S_1 electron pocket versus coverage for Si(111) $\sqrt{3}\times\sqrt{3}$-Au. The data reported in Table II and Figs. 5 and 6 are for a Au coverage of 1.1 ML, which lies in the middle of the range where the $\sqrt{3}\times\sqrt{3}$-Au band topology is observed (1.0–1.2 ML in Fig. 3). At lower coverage the bands move up relative to the Fermi level, and at higher coverage they move down. These shifts are $+0.04$ eV for 1.0 ML Au and -0.13 eV for 1.2 ML Au. The combined shift of 0.17 eV matches the 0.20 eV shift of the bulk Si $2p$ core level between the low-coverage α-$\sqrt{3}\times\sqrt{3}$-Au phase and the high-coverage β-$\sqrt{3}\times\sqrt{3}$-Au phase.[15] This comparison suggests that the filling of the S_1 state determines the Fermi level pinning. Furthermore, our results show that the electronic change between the α and β structures is mainly an increase in band filling, not a change in band topology.

The lower two surface states S_2 and S_3 form an intricate web of bands that is partially obscured by the projected bulk bands. In an attempt to give a best estimate of the band topology we combine our results from Fig. 5 with the dispersion of S_3 near Γ from Ref. 19 and determine a matching set of bands in Fig. 6. The two bands S_2 and S_3 are degenerate at Γ and at the zone boundary M, at least within the uncertainty of about 0.1 eV imposed by the lifetime broadening. Within that uncertainty, they cross over at M such that the S_2 band in the first Brillouin zone becomes the S_3 band in the second Brillouin zone, and vice versa. The double degeneracy of S_2, S_3 at Γ and M suggests a $p_{x,y}$-like character. The simplest $p_{x,y}$ band topology would consist of an upper band S_2 and a lower band S_3 that reach their maximum separation at M and merge at Γ. The double hump around M in our band topology is motivated by the sharp turnaround of the upper band S_2 observed at 1.5 Å^{-1} in Fig. 5, which is clearly different from $M=1.64$ Å^{-1}. Therefore, we require two maxima symmetric about M. These can actually be made out as faint features in the first Brillouin zone. The rest of the S_2, S_3 dispersion follows by replicating the strongest band features from Fig. 5 in the other Brillouin zones and connecting the pieces.

Our bands are consistent with the states S_1, S_2, and S_3 reported previously.[19] In addition to the band extrema, we are able to map out strongly dispersing sections of the bands. We find that S_1 disperses significantly and forms an electron pocket (Fig. 6), whereas its lack of dispersion in Ref. 19 led to an assignment to boundaries between $\sqrt{3}\times\sqrt{3}$ domains. Furthermore, we are able to show that S_2 disperses downward far enough to connect with the maximum of S_3 at Γ, thereby forming a doubly degenerate Γ point.

VI. SUMMARY

In summary, we combine real space information from STM and reciprocal space data from photoemission to obtain insight into the unusual surface states induced by gold at vicinal Si(111) surfaces. It is encouraging to see that metallic bands can be obtained in one-dimensional structures, such as Si(557)-Au. Apparently, the anchoring of the chains to a rigid step lattice counteracts the tendency toward a metal-insulator transition via Peierls distortion. The variety of electronic features that we observe illustrates the potential for tailoring the electronic structure of chains and ladders at stepped surfaces.[34] Several parameters are available for steering a surface toward specific sections of the phase diagram of one-dimensional electrons, such as charge density waves or exotic, non-Fermi liquids. The electron count can be varied by the metal coverage, the coupling between the chains by the step density, the coupling along the chain by the size of the adsorbed atoms, and even the spin structure might be controllable by using magnetic atoms. It is interesting to note that the stripes observed in high-temperature superconductors and other correlated electron systems have widths quite comparable to those of the chain structures for Au on Si(111). A well-defined, static structure of alternating metal-lic and insulating stripes on vicinal Si(111) could become an excellent case for testing theoretical models of stripes.

Before embarking on an ambitious program of tailoring one-dimensional solids we will need to understand the wave

functions underlying their interesting features. First of all, that requires a structure determination coupled with a band structure calculation.[31,32] That will be a challenge for both experiment and theory considering these large, highly reconstructed unit cells. The interplay of single-spaced and double-spaced chains and of Si chains and Au chains is a major unsolved question. Some of the puzzles that we are struggling with now might point toward new models for electronic states.

ACKNOWLEDGMENTS

We are grateful to M. Fisher, C. Gundelach, M. Thikim, and J. Wallace for help with the experimental setup. This work was supported by the NSF under Awards No. DMR-9815416 and No. DMR-0079983. It was conducted at the SRC, which is supported by the NSF under Award No. DMR-0084402.

[1] G. Santoro, S. Scandolo, and E. Tosatti, Phys. Rev. B **59**, 1891 (1999); F. Flores, J. Ortega, and R. Pérez, Surf. Rev. Lett. **6**, 411 (1999).

[2] H. H . Weitering, J. Chen, N. J. DiNardo, and E. W. Plummer, Phys. Rev. B **48**, 8119 (1993); H. H. Weitering, X. Shi, P. D. Johnson, J. Chen, N. J. DiNardo, and K. Kempa, Phys. Rev. Lett. **78**, 1331 (1997); V. Ramachandran and R. M. Feenstra, *ibid.* **82**, 1000 (1999).

[3] J. M. Carpinelli, H. H. Weitering, E. W. Plummer, and R. Stumpf, Nature (London) **381**, 398 (1996); J. M. Carpinelli, H. H. Weitering, M. Bartkowiak, R. Stumpf, and E. W. Plummer, Phys. Rev. Lett. **79**, 2859 (1997).

[4] J. Avila, A. Mascaraque, E. G. Michel, M. C. Asenio, G. Lelay, J. Ortega, R. Pérez, and F. Flores, Phys. Rev. Lett. **82**, 442 (1999); A. Mascaraque, J. Avila, J. Alvarez, M. C. Asensio, S. Ferrer, and E. G. Michel, *ibid.* **82**, 2524 (1999).

[5] S. C. Erwin and H. H. Weitering, Phys. Rev. Lett. **81**, 2296 (1998); F. Pedreschi, J. D. O'Mahony, P. Weightman, and J. R. Power, Appl. Phys. Lett. **73**, 2152 (1998); I. G. Hill and A. B. McLean, Phys. Rev. Lett. **82**, 2155 (1999); H. W. Yeom, S. Takeda, E. Rotenberg, I. Matsuda, K. Horikoshi, J. Schäfer, C. M. Lee, S. D. Kevan, T. Ohta, T. Nagao, and S. Hasegawa, *ibid.* **82**, 4898 (1999).

[6] R. Losio, K. N. Altmann, and F. J. Himpsel, Phys. Rev. Lett. **85**, 808 (2000).

[7] P. Segovia, D. Purdie, M. Hengsberger, and Y. Baer, Nature (London) **402**, 504 (1999).

[8] J. Schäfer, E. Rotenberg, and S. D. Kevan (unpublished).

[9] R. Losio, K. N. Altmann, A. Kiakosian, J.-L. Lin, D. Y. Petrovykh, and F. J. Himpsel, Phys. Rev. Lett. **86**, 4632 (2001).

[10] V. Meden and K. Schönhammer, Phys. Rev. B **46**, 15 753 (1992); J. Voit, Rep. Prog. Phys. **18**, 997 (1995); N. Shannon and R. Joynt, J. Phys.: Condens. Matter **8**, 10 493 (1996); M. G. Zacher, E. Arrigoni, W. Hanke, and J. R. Schrieffer, Phys. Rev. B **57**, 6370 (1998); M. Grioni, I. Vobornik, F. Zwick, and G. Margaritondo, J. Electron Spectrosc. Relat. Phenom. **100**, 313 (1999).

[11] G. LeLay and J. P. Faurie, Surf. Sci. **69**, 295 (1977); L. E. Berman, B. W. Batterman, and J. M. Blakely, Phys. Rev. B **38**, 5397 (1988); A. A. Baski, J. Nogami, and C. F. Quate, *ibid.* **41**, 10 247 (1990); Ch. Schamper, W. Moritz, H. Schulz, R. Feidenhansl, M. Nielsen, F. Grey, and R. L. Johnson, *ibid.* **43**, 12 130 (1991); L. Seehofer, S. Huhs, G. Falkenberg, and R. L. Johnson, Surf. Sci. **329**, 157 (1995); L. D. Marks and R. Plass, Phys. Rev. Lett. **75**, 2172 (1995); M. Shibata, I. Sumita, and M. Nakajima, Phys. Rev. B **57**, 1626 (1998).

[12] L. D. Marks and R. Plass, Phys. Rev. Lett. **75**, 2172 (1995); R. Plass and L. D. Marks, Surf. Sci. **380**, 497 (1997).

[13] J. D. O'Mahony, J. F. McGilp, C. F. J. Flipse, P. Weightman, and F. M. Leibsle, Phys. Rev. B **49**, 2527 (1994).

[14] E. Bauer, Surf. Sci. **250**, L379 (1991).

[15] T. Okuda, H. Daimon, H. Shigeoka, S. Suga, T. Kinoshita, and A. Kakizaki, J. Electron Spectrosc. Relat. Phenom. **80**, 229 (1996).

[16] M. Jalochowski, M. Strozak, and R. Zdyb, Surf. Sci. **375**, 203 (1997).

[17] A. Kirakosian, R. Bennewitz, J. N. Crain, Th. Fauster, J.-L. Lin, D. Y. Petrovykh, and F. J. Himpsel (unpublished).

[18] I. R. Collins, J. T. Moran, P. T. Andrews, R. Cosso, J. D. OMahony, J. F. McGilp, and G. Margaritondo, Surf. Sci. **325**, 45 (1995); for unoccupied states, see I. G. Hill and A. B. McLean, Phys. Rev. B **55**, 15 664 (1997).

[19] C. J. Karlsson, E. Landemark, L. S. O. Johansson, and R. I. G. Uhrberg, Phys. Rev. B **42**, 9546 (1990); for unoccupied states, see J. M. Nicholls, F. Salvan, and B. Reihl, *ibid.* **34**, 2945 (1986).

[20] J. Viernow, J.-L. Lin, D. Y. Petrovykh, F. M. Leibsle, F. K. Men, and F. J. Himpsel, Appl. Phys. Lett. **72**, 948 (1998); J.-L. Lin, D. Y. Petrovykh, J. Viernow, F. K. Men, D. J. Seo, and F. J. Himpsel, J. Appl. Phys. **84**, 255 (1998).

[21] R. Losio, K. N. Altmann, and F. J. Himpsel, Phys. Rev. B **61**, 10 845 (2000); for unoccupied states, see F. J. Himpsel, Surf. Sci. Rep. **12**, 1 (1990). For a 2×2 and $c(4\times2)$ adatom structure the number of adatoms matches that of the rest atoms. That leads to a completely empty adatom band, instead of the partially occupied band on Si(111)7×7.

[22] The branch near $k^{||}=+1.2$ Å^{-1} is better resolved than the other three because this section of the data was taken after a 950 °C anneal, which gave significantly sharper features than the 850 °C anneal used for the rest of the data. Also, the matrix element is particularly high in this region.

[23] L. S. O. Johansson, E. Landemark, C. J. Karlsson, and R. I. G. Uhrberg, Phys. Rev. Lett. **63**, 2092 (1989); X. Tong, C. S. Jiang, and S. Hasegawa, Phys. Rev. B **57**, 9015 (1998); for unoccupied states, see J. Viernow, M. Henzler, W. L. O'Brien, F. K. Men, F. M. Leibsle, D. Y. Petrovykh, J. L. Lin, and F. J. Himpsel, *ibid.* **57**, 2321 (1998).

[24] S. Hawegawa and S. Ino, Phys. Rev. Lett. **68**, 1192 (1992); X. Tong, C. S. Jiang, K. Horikoshi, and S. Hasegawa, Surf. Sci. **449**, 125 (2000).

[25] T. Miller, A. Samsavar, G. E. Franklin, and T.-C. Chiang, Phys. Rev. Lett. **61**, 1404 (1988).

[26] J. N. Crain *et al.* (unpublished).

[27] H. Lipson and K. E. Singer, J. Phys. C **7**, 10 (1974).

[28] STM images shows extra protrusions on top of the chains that randomly occupy lattice sites on Si(111)5×2-Au and Si(557)-Au (see Fig. 2 and Refs. 11 and 13). Such defects comprise about 0.02 ML on Si(111)5×2-Au and 0.01 ML on Si(557)-Au. They appear prominently in the topography, but are outnumbered by the chain atoms in photoemission. For example, the signal from the single band S_1 of Si(111)5×2-Au corresponds to 0.20 ML (one row of five), and for the two bands S_{1A}, S_{1B} of Si(557)-Au to 0.35 ML (two rows of $5\frac{2}{3}$). For Si(111)5×2-Au the contribution of extra atoms is 10% of the Si band, which is comparable to the ratio of the spectral weight in the pseudogap to that of the S_1 band outside the gap.

[29] S. LaShell, B. A. McDougall, and E. Jensen, Phys. Rev. Lett. **77**, 3419 (1996).

[30] R. D. Meade and D. Vanderbilt, Phys. Rev. B **40**, 3905 (1989).

[31] D. Sánchez-Portal J. D. Gale, A. García, and R. M. Martin, cond-mat/0105400 (unpublished).

[32] S. C. Erwin (unpublished).

[33] E. V. Chulkov, P. M. Echenique, A. Liebsch, and F. J. Himpsel (unpublished).

[34] T. Yamada, C. W. Bauschlicher, and H. Partridge, Phys. Rev. B **59**, 15 430 (1999).